Case Report

DOI: 10.3348/kjr.2011.12.2.241
pISSN 1229-6929 · eISSN 2005-8330
Korean J Radiol 2011;12(2):241-246

Korean Journal of Radiology
KJR

Sequential Magnetic Resonance Imaging Finding of Intramedullary Spinal Cord Abscess including Diffusion Weighted Image: a Case Report

Jae Eun Roh, MD, Seung Young Lee, MD, Sang-Hoon Cha, MD, Bum Sang Cho, MD, Min Hee Jeon, MD, Min Ho Kang, MD

All authors: Department of Radiology, Chungbuk National University College of Medicine, Chungbuk 361-711, Korea

Intramedullary spinal cord abscess (ISCA) is a rare infection of the central nervous system. We describe the magnetic resonance imaging (MRI) findings, including the diffusion-weighted imaging (DWI) findings, of ISCA in a 78-year-old man. The initial conventional MRI of the thoracic spine demonstrated a subtle enhancing nodule accompanied by significant edema. On the follow-up MRI after seven days, the nodule appeared as a ring-enhancing nodule. The non-enhancing central portion of the nodule appeared hyperintense on DWI with a decreased apparent diffusion coefficient (ADC) value on the ADC map. We performed myelotomy and surgical drainage, and thick, yellowish pus was drained.
Index terms: *Intramedullary spinal cord abscess; Magnetic resonance imaging; Diffusion-weighted imaging*

INTRODUCTION

Intramedullary spinal cord abscess (ISCA) is a well recognized, but rare entity (1). Since the original description by Hart in 1830, fewer than 120 cases have been reported in the literature (2, 3). Making an early diagnosis according to a clinical suspicion and the radiological findings are essential and then administering appropriate antibiotic therapy and surgical intervention are crucial to reduce the mortality and neurological sequelae. Several cases of ISCA were reported with the magnetic resonance imaging (MRI) findings in the previous literature, but to the best of our knowledge, only one case that was diagnosed as ISCA based on diffusion-weighted MR imaging has been reported (1). We report here on the sequential MRI and diffusion-weighted image (DWI) findings of a case of surgically proved ISCA.

CASE REPORT

A 78-year-old man presented with the sudden onset of drowsiness, weakness in both legs and a four day history of back pain, fever, chills and myalgia. He had been diagnosed with alcoholic liver cirrhosis and hepatocellular carcinoma (HCC) with omental metastasis about five years earlier, and he had been treated with transarterial chemoembolization (TACE) for the HCC and colon resection for the metastatic HCC. He had been taking drugs for diabetes mellitus for 20 years. On admission, he was confused and afebrile. The clinical examination revealed flaccid paraplegia and complete sensory loss, except for light touch, below the level of T4. The deep tendon jerks were normoactive in the bilateral arms and they were absent in the bilateral legs. On blood testing at admission, the white blood cell count (9900/μL) was normal and the C-reactive protein level (4.33

Received July 2, 2010; accepted after revision October 1, 2010.
Corresponding author: Seung Young Lee, MD, Department of Radiology, Chungbuk National University College of Medicine, 410 Seongbong-ro, Heungduk-gu, Cheongju-si, Chungbuk 361-711, Korea.
• Tel: (8243) 269-6472 • Fax: (8243) 269-6479
• E-mail: lsyrad@chungbuk.ac.kr

mg/dL) was slightly elevated. Analysis of the cerebrospinal fluid (CSF) specimens on lumbar puncture revealed that the white blood cell count was 640/μL (50% polymorphonuclear cells), the red blood cell count was 170/μL, the protein level was 357.1 mg/dL and the glucose level was 158 mg/dL. Blood cultures revealed *Listeria monocytogenes*. MRI of the brain and thoracic spine were performed using a 3.0T scanner (Achieva X-series, Philips, Best, The Netherlands). The brain MRI did not show any acute inflammatory or infectious lesions, except for diffuse brain atrophy and multifocal chronic ischemic lesions in the bilateral cerebral hemispheres. The thoracic spine MRI demonstrated intramedullary nodular high signal intensity at the T9 level accompanying the surrounding edema and mild swelling of the spinal cord from the T7 to T11 level on the T2-weighted images (T2WI). T1-weighted imaging (T1WI) after gadolinium injection showed subtle spotty enhancement within the nodule at the T9 level (Fig. 1A-C). Our initial differential diagnosis was demyelinating disease such as transverse myelitis or acute disseminated encephalomyelitis (ADEM), and metastasis was also considered because of his underlying malignancy. On the basis of patient's symptoms, blood and CSF tests, meningitis or hidden infection was considered. The patient was treated with empirical intravenous antibiotics, including ampicillin (2 g every 4 h), vancomycin (1 g every 12 h) and cefotaxime (2 g every 12 h), and acyclovir (700 mg every 8 h) and dexamethasone because we could not rule out the possibility of metastasis. Three days after admission, he became alert, but his paraplegia did not improve. Follow-up MR imaging of the thoracic spine, which was performed 10 days after the initial presentation, showed an increased extent of intramedullary high signal intensity and aggravated swelling from the T5 to T11 level. The size of the nodular lesion at the T9 level was also increased and the nodular lesion had changed to a discrete nodule with accompanying intense peripheral rim enhancement on the fat-saturated T1WI after intravenous gadolinium injection (Fig. 1D-H). We acquired additional DWIs on the sagittal plane with a b-value of 600 s/mm^2 to differentiate an abscess from a tumor. The non-enhancing cavity of the nodule at the T9 level appeared hyperintense on DWI and there were decreased apparent diffusion coefficients (ADCs) on the ADC map as compared with the adjacent spinal cord (Fig. 1I, J). Regions of interest (ROI) were drawn within the abscess cavity, the adjacent edema and the normal-appearing spinal cord (Fig. 1K) on the ADC map. The measured ADC values were 0.610 × 10^{-3} mm^2/s in the abscess cavity, 1.306 × 10^{-3} mm^2/s in the swollen spinal cord and 1.143 × 10^{-3} mm^2/s in the normal-appearing spinal cord. On the basis of the decreased diffusivity in the cavity on DWI and the rapid progression, we presumed that the diagnosis was ISCA rather than a spinal cord tumor such as metastasis.

The patient underwent surgical drainage because of

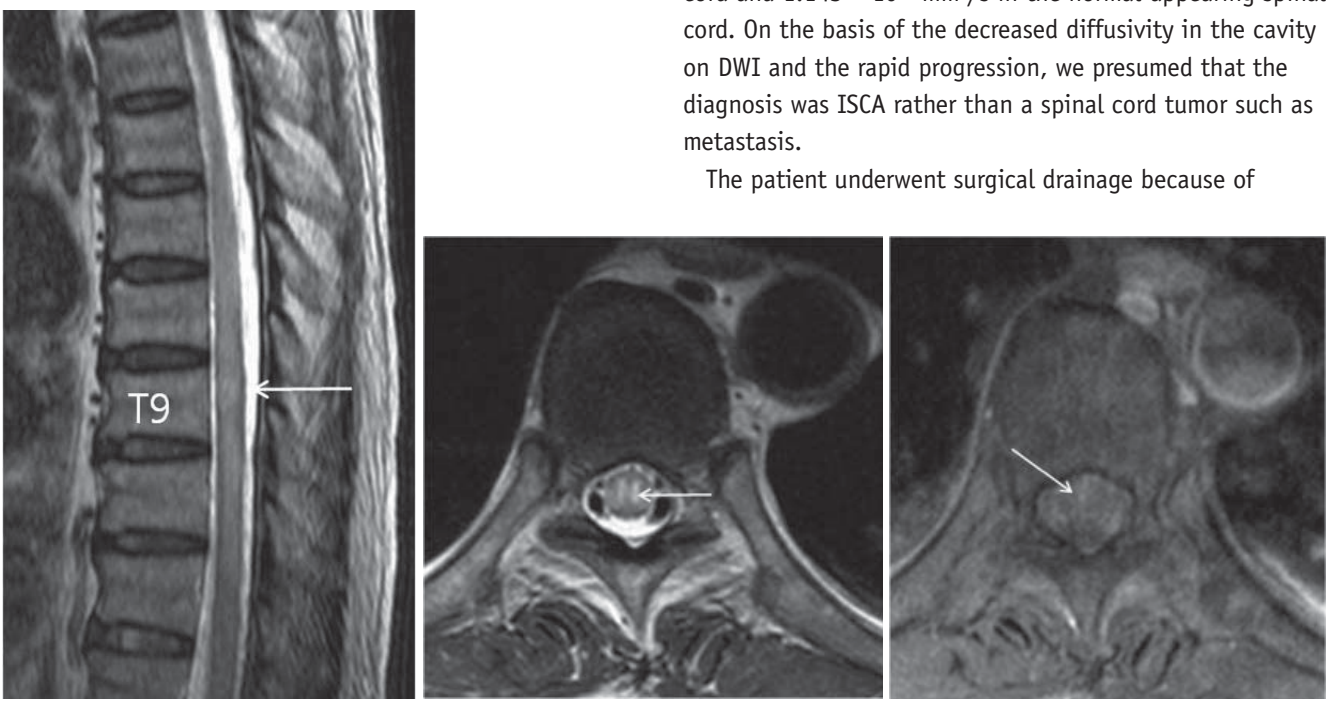

A B C

Fig. 1. Intramedullary spinal cord abscess in 78-year-old man.
A-C. Initial MRI of thoracic spine shows focal hyperintense nodular lesion involving gray matter at level of T9 (arrows) and diffuse intramedullary high signal intensity extending from T7 to T11 on sagittal (**A**) and axial (**B**) T2-weighted images. Axial fat-saturated T1-weighted image with gadolinium (**C**) at level of T9 shows focal spotty intramedullary enhancement (arrow in **C**).

Korean Journal of Radiology
KJR

his afebrile back pain and persistent paraplegia. A total laminectomy at the T8-9 level was performed and the dura was opened. The atrophic spinal cord was seen through the durotomy. On myelotomy, a yellowish, purulent fluid ran out, and this was followed by copious irrigation with normal saline (Fig. 1L). The pathology revealed no malignant cells in the abscess materials and the culture of the pus aspirate was negative. The antibiotics were continued with a combination of ampicillin and cefotaxime based on the blood culture sensitivity.

Follow-up MR imaging performed two weeks after the surgical treatment showed an improved intramedullary signal change and enhancement and a decreased extent of spinal cord edema, but there was a residual enhancing nodule at the T9 level. A localized posterior epidural fluid collection and ill defined enhancement at the posterior paraspinal area suggesting postoperative change at T8-10 level were also noted (Fig. 1M-O). However, the patient's symptoms did not improve and his paraplegia persisted at the two month assessment.

DISCUSSION

Intramedullary spinal cord abscess is a rare condition since the normal spinal cord tissue has remarkably high resistance to infection. The etiology of this condition is variable. Those cases reported in recent times have usually been cryptogenic in origin (4). Many cryptogenic cases have

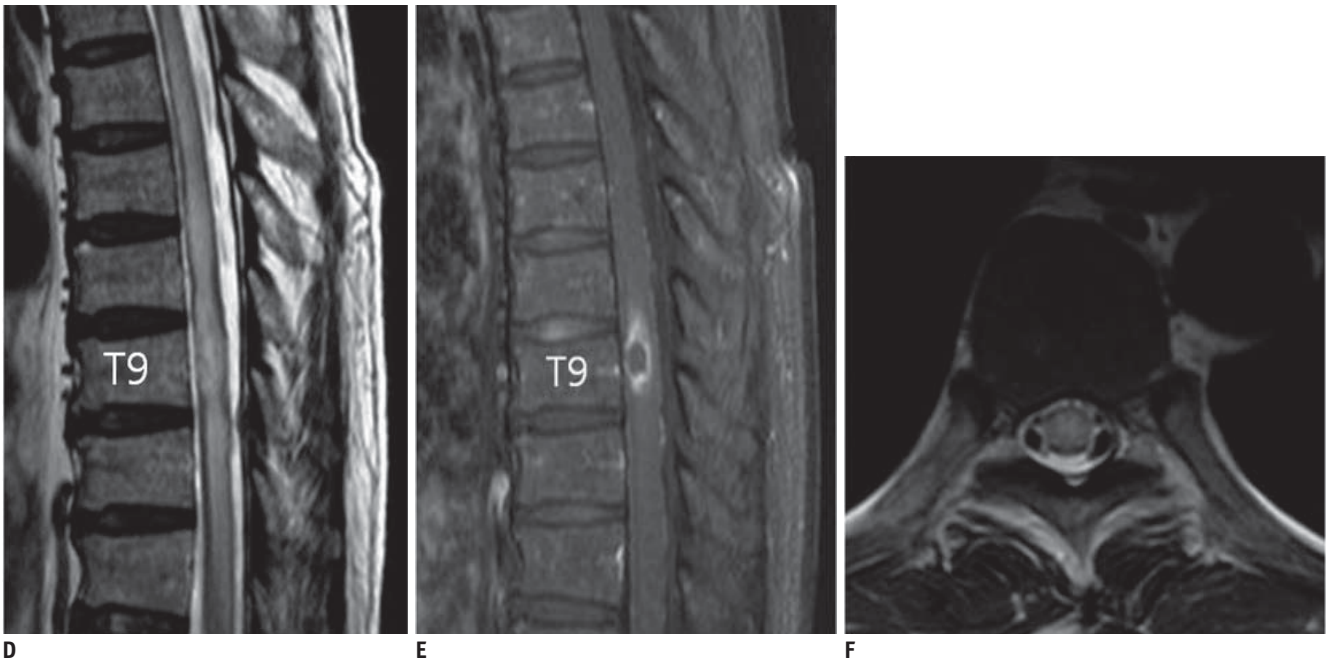

Fig. 1. Intramedullary spinal cord abscess in 78-year-old man.
D-H. Follow-up MRI of thoracic spine that was performed 10 days after initial presentation shows more prominent focal hyperintense lesion at T9 level and increased extent of intramedullary hypersignal intensity, and this all suggested edema from T5 to T11 on sagittal (**D**) and axial (**F**) T2-weighted images. Fat-saturated sagittal T1-weighted image after gadolinium injection (**E**) shows intramedullary ring-enhancing lesion at T9 level. Precontrast (**G**) and postcontrast (**H**) axial T1-weighted MRI at T9 level show striking intramedullary enhancement.

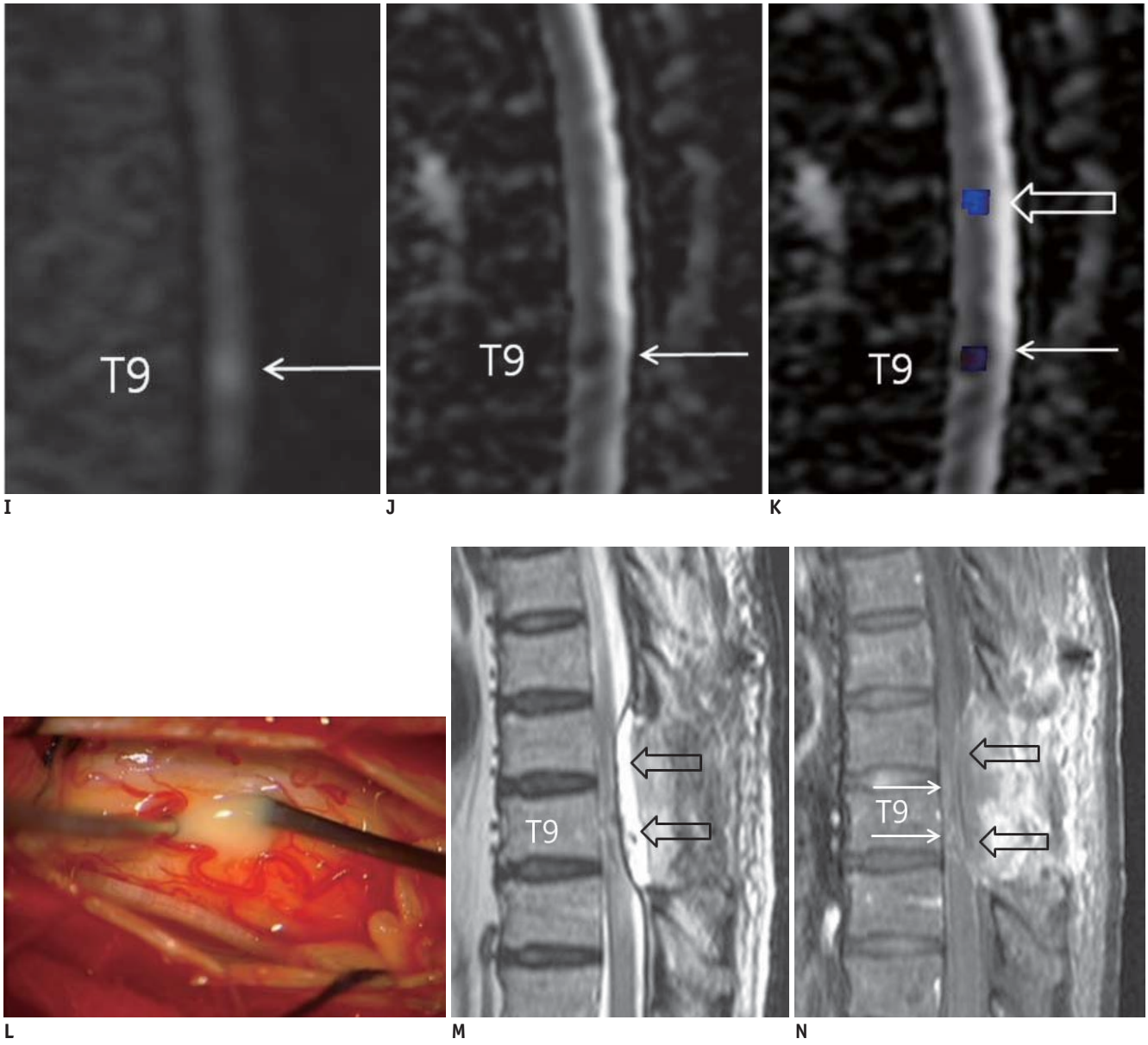

Fig. 1. Intramedullary spinal cord abscess in 78-year-old man.
I. Sagittal diffusion-weighted imaging shows intramedullary hyperintensity at T9 level (arrow). **J.** Sagittal apparent diffusion coefficient map shows restricted apparent diffusion coefficient map at T9 level (arrow). **K.** Apparent diffusion coefficient map with region of interest shows each apparent diffusion coefficient value in abscess cavity, surrounding edema and normal spinal cord. Apparent diffusion coefficient within region of interest measured 0.610 × 10^{-3} mm^2/s in abscess cavity (arrow), 1.306 × 10^{-3} mm^2/s in surrounding edema (open arrow) and 1.112 × 10^{-3} mm^2/s in normal-appearing spinal cord (not shown). **L.** Intraoperative photograph shows yellowish pus after myelotomy at T8-9 level. **M-O.** Follow-up MRI of thoracic spine performed two weeks after surgical treatment shows markedly improved intramedullary signal change and spinal cord swelling on sagittal (**M**) T2-weighted images and at-saturated postcontrast sagittal (**N**) and axial (**O**) T1-weighted images. But there was residual increased intramedullary signal intensity and contrast enhancement (arrows) at T9-10 level. Postoperative epidural fluid collection (open arrows) and ill-defined enhancement at posterior paraspinal area from T8 to T10 level were also noted.

Korean Journal of Radiology
KJR

originated from transient bacteremia transferred from the mucosal surfaces or from clinically unrecognized extraspinal sites of infection (3). Metastatic abscess and extension from adjacent structures are also mechanisms of infection (4, 5). Congenital midline defects and anatomic abnormalities of the spinal cord or vertebral column are predisposing factors in pediatric ISCA (3, 5). Other causes are direct trauma or neurosurgical intervention (1).

Although 30% of cases are microbiologically sterile, various organisms have been isolated, including *Staphylococcus, Streptococcus pneumonia, Haemophilus, Proteus, Listeria, Actinomyces, Pseudomonas cepacia* and *Mycobacterium tuberculosis* (6). In our case, although the blood culture revealed listeriosis, we could not find the origin of the infection. *Listeria monocytogenes* most commonly causes central nervous system infections, including meningitis, encephalitis, rhombencephalitis, brain abscesses and spinal cord disease (7). The risk factors for developing listeriosis are organ transplantation, hematologic malignancy, acquired immune deficiency syndrome (AIDS), pregnancy, liver failure, solid organ malignancy, diabetes mellitus and an age older than 60 years (7). Old age and long-standing diabetes mellitus were probable risk factors for our patient.

The clinical presentations of ISCA are motor and sensory deficits (68%), urinary incontinence (56%), fever (40%), meningismus (12%) and brain stem dysfunction (4%) (4). The triad of ISCA is fever, pain and neurological deficits, but this does not occur in all patients (3). The clinical findings of ISCA are nonspecific and they do not lead to a final diagnosis. For therapy, it is most important to differentiate ISCA from other tumorous conditions in order to promptly initiate adequate medical and surgical treatment.

The radiologic technique of first choice is MRI with intravenous gadolinium to accurately determine the location and size of an intramedullary abscess, and to identify any predisposing structural abnormalities of the spinal cord or vertebral body (3, 5). The MRI features of ISCA include increased signal intensity on T2WI and marginal enhancement with central low signal intensity on T1WI with gadolinium (3). A ring-enhancing mass is a nonspecific imaging finding, and a variety of non-inflammatory benign and neoplastic processes can have a similar appearance (1). The differential diagnosis of a ring-enhancing mass includes primary or secondary cord tumors (necrotic glioma, metastases), resolving hematoma, infarction and demyelinating disease (1).

Diffusion-weighted imaging has been added to the diagnostic imaging techniques in recent years and it has been recommended as a more sensitive and specific method for differentiating abscesses from cystic or necrotic cerebral tumors (8). For cerebral pathology, DWI is frequently used for examining ischemic, infectious, inflammatory, tumoral and hemorrhagic diseases (9). DWI can be helpful in clinically atypical acute myelopathies to distinguish spinal cord infarction from inflammatory myelopathies such as multiple sclerosis, ADEM, neuromyelitis optica and parainfectious myelopathy (9). However, there has been only one report that has described the diagnostic value of DWI and ADC in ISCA (1).

Diffusion-weighted imaging is based on the microscopic motion of water molecules and it mostly depends on the water located in the extracellular space, for example, in brain parenchyma, tumor tissue, pus or cysts (8, 10). Like brain abscesses, the high signal intensity of abscess pus on a DWI scan that is associated with a low ADC can help to distinguish ISCA from cystic spinal cord tumors (8). Increased DWI signal intensity is noted in abscess cavities as compared to that in normal brain parenchyma, which reflects restricted diffusion, whereas the signal intensity is generally hypointense in tumor cysts and necrosis, which reflects more isotropic diffusion, such as in CSF (8).

Necrotic materials in abscesses contain inflammatory cells, a matrix of proteins, cellular debris and bacteria in high-viscosity pus; all of these factors restrict water motion (10). Additionally, water molecules are bound to carboxyl-, hydroxyl- and amino-groups on the surface of macromolecules and this further restricts their motion. Therefore, restricted water motion in an abscess leads to increased signal intensity on DWI and low ADC values (10). We measured each of the ADC values in the abscess cavity, the surrounding edema and the normal-appearing spinal cord. The ADC value in the abscess cavity was decreased relative to the normal spinal cord (0.610×10^{-3} mm^2/s vs. 1.143×10^{-3} mm^2/s, respectively), and this represented decreased water diffusivity.

Similar to the management of pyogenic brain abscesses, a combination of medical and surgical therapies is recommended for the treatment of ISCA. Diagnostic and therapeutic drainage of the abscess may be accomplished through an open surgical approach (myelotomy) or by stereotactic needle aspiration of the lesions under CT guidance (4). Empirical antimicrobial therapy should be based on the presumed mechanism of infection and the

results of gram staining of the aspirate (4). Our patient underwent surgical drainage because his afebrile back pain and neurologic deficit did not improve. We performed myelotomy and pus drainage, but his paraplegia did not improve.

REFERENCES

1. Dörflinger-Hejlek E, Kirsch EC, Reiter H, Opravil M, Kaim AH. Diffusion-weighted MR imaging of intramedullary spinal cord abscess. *AJNR Am J Neuroradiol* 2009;31:1651-1652
2. Hart J. Case of encysted abscess in the center of the spinal cord. *Dublin Hospital Report* 1830;5:522-524
3. Kurita N, Sakurai Y, Taniguchi M, Terao T, Takahashi H, Mannen T. Intramedullary spinal cord abscess treated with antibiotic therapy-case report and review. *Neurol Med Chir (Tokyo)* 2009;49:262-268
4. Chan CT, Gold WL. Intramedullary abscess of the spinal cord in the antibiotic era: clinical features, microbial etiologies, trends in pathogenesis, and outcomes. *Clin Infect Dis* 1998;27:619-626
5. Al Barbarawi M, Khriesat W, Qudsieh S, Qudsieh H, Loai AA. Management of intramedullary spinal cord abscess: experience with four cases, pathophysiology and outcomes. *Eur Spine J* 2009;18:710-717
6. Hung PC, Wang HS, Wu CT, Lui TN, Wong AM. Spinal intramedullary abscess with an epidermoid secondary to a dermal sinus. *Pediatr Neurol* 2007;37:144-147
7. Clauss HE, Lorber B. Central nervous system infection with Listeria monocytogenes. *Curr Infect Dis Rep* 2008;10:300-306
8. Reiche W, Schuchardt V, Hagen T, Il'yasov KA, Billmann P, Weber J. Differential diagnosis of intracranial ring enhancing cystic mass lesions--role of diffusion-weighted imaging (DWI) and diffusion-tensor imaging (DTI). *Clin Neurol Neurosurg* 2010;112:218-225
9. Marcel C, Kremer S, Jeantroux J, Blanc F, Dietemann JL, De Sèze J. Diffusion-weighted imaging in noncompressive myelopathies: a 33-patient prospective study. *J Neurol* 2010;257:1438-1445
10. Cartes-Zumelzu FW, Stavrou I, Castillo M, Eisenhuber E, Knosp E, Thurnher MM. Diffusion-weighted imaging in the assessment of brain abscesses therapy. *AJNR Am J Neuroradiol* 2004;25:1310-1317